IEEE Access
Multidisciplinary ⋮ Rapid Review ⋮ Open Access Journal

Received 23 February 2025, accepted 9 March 2025, date of publication 18 March 2025, date of current version 25 March 2025.

Digital Object Identifier 10.1109/ACCESS.2025.3552023

TOPICAL REVIEW

Application of Metamaterials in Antennas for Gain Improvement: A Study on Integration Techniques and Performance

MD MIRAZUR RAHMAN[1], YANG YANG[2], (Senior Member, IEEE), AND SHUVASHIS DEY[1], (Member, IEEE)

[1]Department of Electrical and Computer Engineering, North Dakota State University, Fargo, ND 58105, USA
[2]School of Electrical and Data Engineering, University of Technology Sydney, Ultimo, Sydney, NSW 2007, Australia

Corresponding author: Shuvashis Dey (Shuvashis.dey@ndsu.edu)

This work was supported by United States Department of Agriculture (USDA) under Grant FAR0037087.

ABSTRACT Metamaterials, with their extraordinary electromagnetic properties, have transformed antenna design by offering advanced control over signal propagation and radiation patterns. This review emphasizes on the integration techniques of major types of metamaterials in antennas to achieve significant gain enhancement. It begins with an overview of metamaterials, discussing their distinct types, properties, and the fundamental principles that enable them to manipulate electromagnetic waves in novel ways. The review then delves into the core topic: the application of these major types of metamaterials in enhancing antenna gain. It thoroughly examines four primary integration techniques, detailing the physical structures. Furthermore, the review analyses how specific metamaterials are integrated with different antennas along with their performances in terms of gain enhancement. Additionally, the review briefly addresses the current challenges and limitations in the existing techniques of integration of metamaterials with antennas in the context of recent advancements, emphasizing scopes for future research in order to fully exploit the potential of metamaterial-enhanced antennas.

INDEX TERMS Metamaterial, antenna, gain enhancement, metamaterials integration, metalens, GRIN lenses.

I. INTRODUCTION

Antennas are characterized by several key parameters amongst which gain is significantly related to any antenna's performance. Antenna gain quantifies an antenna's capacity to focus or concentrate radio frequency energy in a particular direction or pattern, relative to a source that emits radiation equally in all directions [1]. The signal strength of a wireless communication system is commonly measured in terms of gain and plays a crucial role in determining both the effective range and the quality of the system.

Metamaterials, a class of engineered materials with unique electromagnetic properties, have opened new possibilities in antenna design and performance enhancement. These materials possess exotic properties not found in naturally occurring substances, enabling precise control over electromagnetic waves [2]. Metamaterial equipped antenna systems are widely studied for improving gain by maneuvering the radiation properties of an antenna. However, there are challenges in reaching a point where both gain and the profile of the antenna system is equally acceptable when the gain of antenna is the point of interest. Enhancing an antenna's size and gain simultaneously is challenging due to physical and design constraints. For example, although metalenses can increase gain, they often add to the antenna's size. Similarly, adding more unit cells increases gain at the expense of the overall size of the antenna. In addition, advanced metasurface/lenses are offering solutions with superior gain but their complexities pose serious challenges in terms of fabrication and costs. Overall, achieving optimal performance largely depends on the effective integration techniques of the suitable metamaterials with the aforementioned approaches, this

The associate editor coordinating the review of this manuscript and approving it for publication was Li Yang.

section provides a structural analysis of the major techniques for integrating metamaterials into antennas. It then examines different types of antennas integrated with metamaterials within the context of these techniques. The entire analysis focuses on structural aspects and performance improvements, specifically how different integration methods and metamaterials contribute to gain enhancement of antennas. The key contributions of this review include:

- A brief study on metamaterials, covering their fundamental types, and characteristics, and working principles based on cutting-edge literature.
- An extensive structural analysis on various methods for integrating metamaterials with antennas to boost gain, along with an evaluation of their effectiveness.
- An extended structural and performance analysis on previously mentioned integration techniques in the context of different metamaterial-integrated antennas.
- A summary on the existing research gaps and limitations of the aforementioned metamaterial-equipped antennas, along with suggestions for future research directions.

The rest of the paper is organized as follows: Section II covers the fundamentals and basic principles of metamaterials. Section III provides a critical analysis of the structures and performance of different integration techniques of metamaterials and metamaterial-based antennas for gain enhancement. A summary of future challenges and research directions is presented in Section IV, and Section V concludes the paper.

II. FUNDAMENTALS OF METAMATERIALS

Metamaterials are engineered, man-made structures with unique electromagnetic properties not found in natural materials. These include the ability to manipulate dispersion which results unusual permittivity and permeability eventually leading to negative index [3]. The relationship between refractive index, effective electric permittivity (ε_{eff}) and magnetic permeability (μ_{eff}) can be shown as [4],

$$n = \sqrt{\pm\varepsilon_{eff}\,\mu_{eff}} \tag{1}$$

where n denotes the index of refraction.

The constitutive parameters of these materials, such as permittivity and permeability, depend on the spacing between cells and the geometric shape of the unit cell, which are typically implemented on a planar substrate [5].

Metamaterials are fundamentally classified into several categories based on their permittivity and permeability values: Epsilon-Negative (ENG), Double Negative (DNG), Mu-Negative (MNG), and Double-Positive (DPS) materials where all the four regions are depicted in Fig. 1 [6]. DPS materials, known for isotropic dielectrics and right-hand materials, have both positive permeability and permittivity, being considered as conventional material.

A. MATERIALS WITH NEGATIVE PERMITIVITY

ENG metamaterials are engineered to have negative permittivity as shown in ENG region (Fig. 1). This is achieved

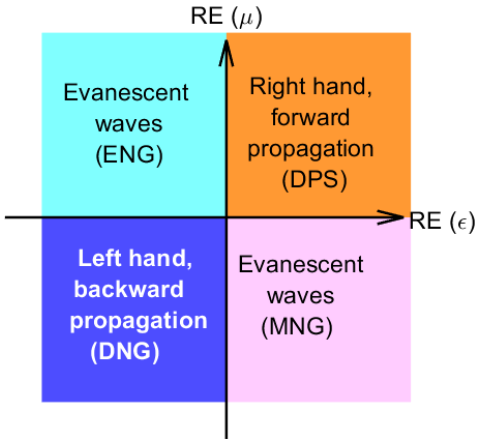

FIGURE 1. Four fundamental regions based on material's permittivity and permeability values. Four quadrants signify four basic types [6].

through the design of subwavelength structures, such as thin metallic wires that interact with electromagnetic fields at specific frequencies. A structure containing thin conductive wires with radius of α, arranged in a periodic array with periodicity of p as shown in Fig. 2 (a) can exhibit negative permittivity [4] as in,

$$\varepsilon_{eff}\,(\omega) = 1 - \frac{\omega_p^2}{(\omega)^2} \tag{2}$$

where ω_p is the plasma frequency and defined as,

$$\omega_p^2 = \frac{2\pi c^2}{p^2 ln\left(\frac{p}{\alpha}\right)} \tag{3}$$

The corresponding permittivity response (Fig. 2 (a)) shows negative real part of effective permittivity below the plasma frequency.

B. MATERIALS WITH NEGATIVE PERMEABILITY

MNG materials are designed with a permeability (μ) negative and used in ferromagnetic and ferrite materials. Negative permeability is normally achieved using resonant magnetic elements like split-ring resonators or other intricate magnetic structures as shown in Fig. 2 (b) at a subwavelength scale. The effective permeability exhibited by this type of resonator is given by,

$$\mu_{eff}\,(\omega) = 1 - \frac{A\omega^2}{\omega^2 - \omega_m^2 + j\omega\Gamma_m} \tag{4}$$

Here A and Γ_m are the damping parameters and the function of geometric parameters of s, g, w of the resonator at resonating frequency (ω_m) [4].

C. MATERIALS WITH BOTH NEGATIVE PERMITIVITY AND PERMEABILITY

DNG metamaterials are perhaps the most intriguing, as they exhibit both permittivity and permeability less than zero or negative [7]. They are known as left handed materials

being able to generate backward wave propagation. This can be realized through a combination of electric and magnetic resonant structures, such as paired split-ring resonators and wire strips, which are carefully designed to achieve negative permittivity and permeability simultaneously [8]. The first ever DNG structure (Fig. 3) as the combination of wires and SRRs was developed by [9].

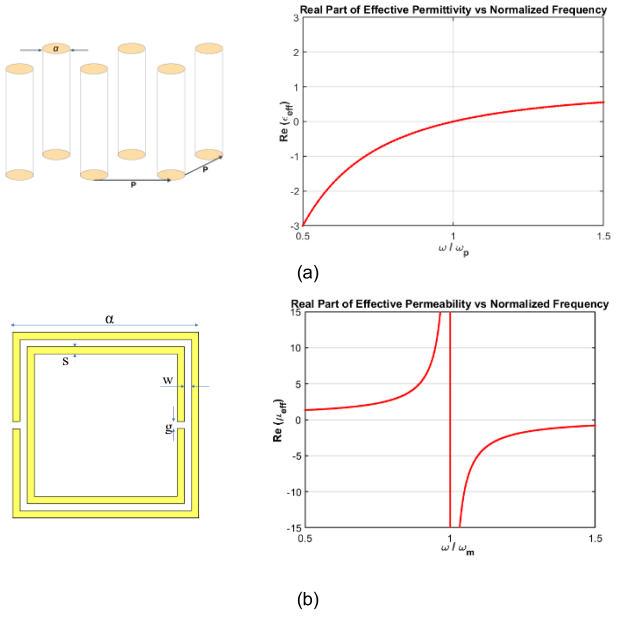

FIGURE 2. Realization of ENG and MNG materials. (a) Array of thin metallic wire (left) with real part of effective permittivity (right), and (b) an SRR unit cell (left) along with the real part of effective permeability (right).

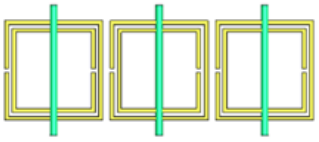

FIGURE 3. Thin metallic wire is placed in front of SRRs to realize a DNG material.

III. METAMATERIAL INTEGRATION INTO ANTENNAS FOR GAIN IMPROVEMENT

In this part, a thorough analysis on integration of metamaterials has been conducted. To facilitate understanding, this section initially provides a structural analysis of the major techniques for integrating metamaterials into antennas. It then examines different types of antennas integrated with metamaterials based on the aforementioned integration techniques. The entire analysis focuses on structural aspects and performance improvements, specifically how different integration methods and antenna systems contribute to gain enhancement.

A. INTEGRATION TECHNIQUES

The effectiveness of metamaterials in improving antenna performance hinges on their integration techniques. These methods exploit metamaterials' distinctive electromagnetic properties, like negative refractive index, high impedance surfaces, and electromagnetic bandgap structures, to overcome particular challenges in antenna design. The selection of an integration approach is influenced by the targeted antenna types, operating frequency, and specific application requirements [10]. The loading or integration of metamaterials with antenna, in order to enhance gain, can be broadly classified as followings whereas Fig. 4 exhibits generic overviews of four types of major metamaterial integration techniques.

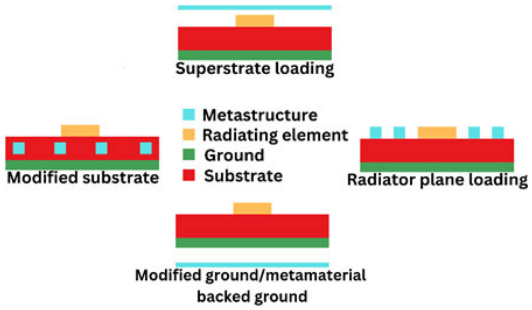

FIGURE 4. A generic representation of four major types (radiator/patch loading, ground plane loading, substrate loading and superstrate loading) of metamaterial loading with antenna.

1) RADIATOR LOADING

In typical scenarios, metamaterial structures or cells are integrated with the antenna, referred to as meta-resonators, or they are arranged, on the top of substrate (coplanar with the radiator). This placement near or on the radiator is especially beneficial for achieving antenna miniaturization and compactness. Additionally, this coplanar arrangement of meta-structures and the radiator simplifies the integration process compared to other methods. In literature, there are myriad of investigations on different ways to place metamaterial structures coplanar with the radiator. For instance, a 3×6 array of metamaterial unit cells is positioned on the substrate of a wideband directional conformal antenna. The cells' low index property leads to a higher phase velocity relative to other regions, enabling the structure to function as a beam-focusing lens with a peak gain of 6.5 dB [11]. study [12] incorporates a diagonal pattern of modified split-ring resonators (SRR) into the same plane as the dual-band microstrip antenna's radiator (Fig. 5). This study examines the gain variations with different loading types near the radiator, finding that a diagonal pattern with increased unit cells significantly boosts gain.

This setup also improves gain in the lower WLAN band (2.4–2.484 and 5.15–5.85 GHz) without affecting the upper band's characteristics. Similarly, the study [13] shows a substantial gain improvement from −0.5 dB to 3.63 dB at

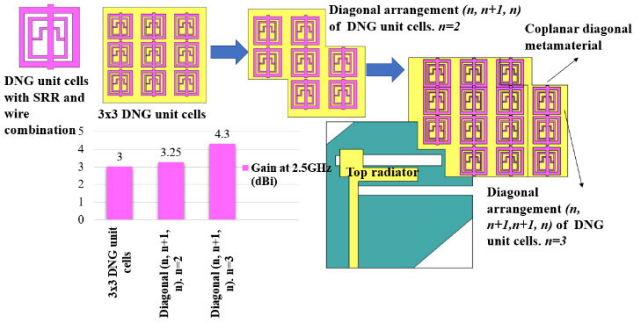

FIGURE 5. Diagonally loading of unit cells on/near radiator with increasing number enhances gain of a dual band microstrip antenna [12].

2.36 GHz in a reference antenna after adding a 3 × 5 array of modified SRR. This improvement is particularly relevant as it addresses the challenge of low or negative gain in lower frequency bands, a critical concern in antenna design and electromagnetic applications [14],. Another innovative approach in [16] involves using an array of square-shaped resonators with diagonal cross- slots (SSDCR) on the ground plane and adding triangle-shaped capacitive coupled resonators (TSCCR) on the patch. Increasing the number of these unit cells enhances the microstrip patch antenna's gain and broadband operability, as shown in Fig. 6 [16].

2) GROUND PLANE LOADING

Metamaterial ground planes, known for their unique electromagnetic properties such as high impedance or artificial magnetic conductivity, are increasingly being used in antenna designs. They enhance radiation patterns, improve impedance matching, minimize back radiation, and overall, boost antenna gain [17]. Metasurfaces like AMCs and EBGs are particularly preferred for ground planes due to their reflective and zero phase-shifting properties, which are discussed later in the review. Integrating these metamaterial ground planes into antennas requires precise design to align with the antenna's frequency and radiation characteristics [18], proving particularly useful for achieving higher gain without sacrificing miniaturization [19]. Generally, the integration can either be as an etched-out ground with periodic structures as shown in Fig. 7 (a) or an additional metamaterial plane is placed close to the ground of an antenna (Fig. 7 (b)). The lattice of SRR and CSRR etched from the ground plane described in [20] can be used for optimizing antenna's performance through adjustments in capacitance and inductance values. This design achieves negative ε and μ at 5.8 GHz and is implemented in a 2×4 MIMO system, yielding a peak gain of 9.2 dB. This approach normally eliminates the requirement of embedding additional structures, instead utilizes the ground itself as a metasurface. As a different approach from the previous one, as [21] illustrates, an Ultra-Wide Band (UWB) microstrip patch antenna's ground can be backed by a metamaterial reflector to reduce back radiation and further enhance gain. Here, the gain is significantly influenced by the gap between the reflector and the antenna, as depicted in Fig. 7 (b).

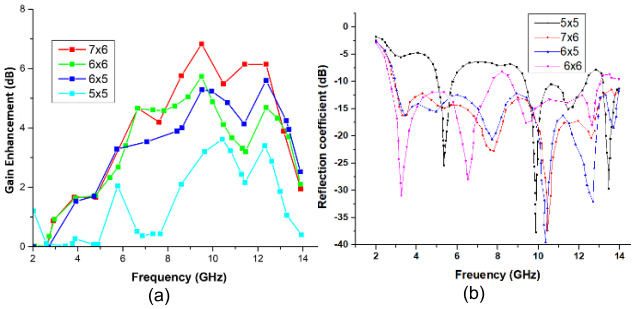

FIGURE 6. Number of elements in the array of the unit cells of metamaterial (a) affects gain, and (b) broadband operability significantly [16].

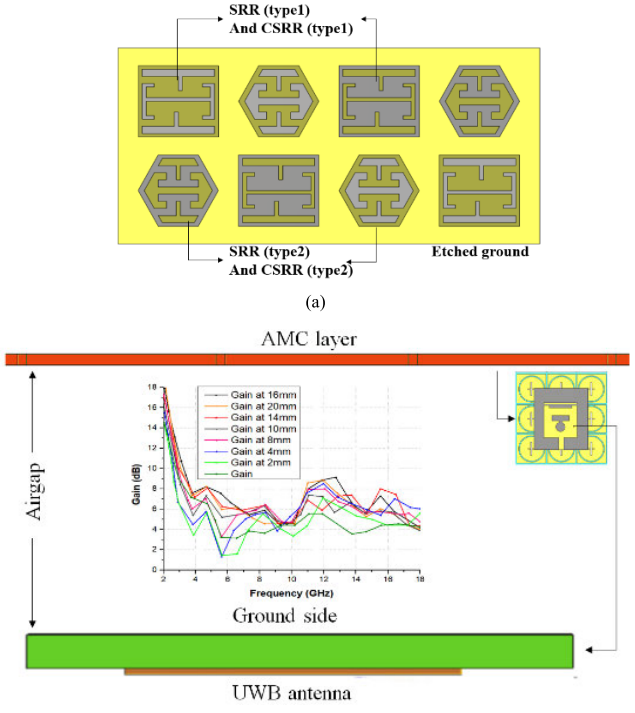

FIGURE 7. (a) The etched-out ground with an array of SRR and CSRR [20], and(b) variation of gain with distance between antenna and metamaterial reflector in the case when ground is backed by the reflector [21].

3) SUBSTRATE LOADING

Embedding metamaterials into substrates is a method for altering dielectric properties to boost antenna gain. In [22], microstrip patch antenna (MPA) incorporates a Capacitive Loaded Loop (CLL) metamaterial unit cell arrangement. The MPA construction uses two FR4 slabs. One slab features the metamaterial cell array on one side and copper laminate on

the other, while the second slab has the antenna patch on one side and no copper laminate on the opposite side. These slabs are stacked such that the metamaterial cell array is positioned between the antenna patch and the ground plane (Fig. 8).

Another example is in [23] where a 4 × 4 U–T DNG metamaterial array is embedded in the middle of a rectangular microstrip patch antenna's substrate, designed for the C-band. This careful placement of the metamaterial array leads to enhanced antenna performance, including an 18% gain increase and a 24% boost in directivity. The strategic positioning of the metamaterial within the substrate is the key, enabling the antenna to retain its original radiation while benefiting from the metamaterial's unique properties. Improvement of gain in antennas through integrating metamaterials into substrates is not yet well explored.

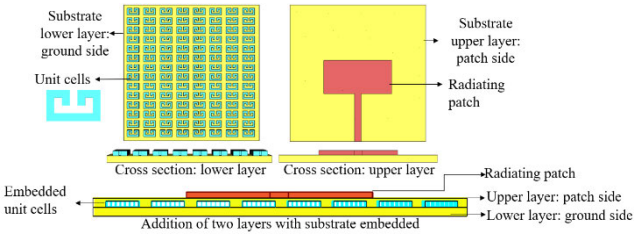

FIGURE 8. Array of metamaterial unit cells immersed into substrate acting as a modified substrate [22].

4) SUPERSTRATE LOADING

A superstrate, placed above or in front of an antenna's radiating element, can manipulate electromagnetic waves in unique and powerful ways. This enhanced capability allows the superstrate to bend or focus electromagnetic waves more effectively, improving the antenna's performance and efficiency. According to existing literatures, the main objective of using metamaterial superstrates is to boost the antenna's gain, employing them as a standard single or multilayer lens (metalens). The superstrate's thickness, number of layers, and number of unit cells in each layer should be tailored to match the antenna's specific frequency and radiation properties. The spacing between the superstrate and the radiating element is another vital aspect, influencing the interaction of electromagnetic waves with the superstrate. It is suggested that the superstrate be placed at a height where near-field coupling with the substrate and radiating elements is minimized [24]. Additionally, the optimal height can enhance gain by maximizing the cavity effect due to high reflectivity. To determine the ideal superstrate height and the unit cell spacing, a parametric study is conducted in [25]. This study introduces a two-element MIMO antenna with a 4 × 2 array of DNG unit cells as a superstrate. Integrating metamaterials as superstrates can be especially beneficial in scenarios requiring substantial gain and directivity enhancement without considerably enlarging the antenna's physical size.

Table 1 summarizes various metamaterial integration techniques and their corresponding performance outcomes

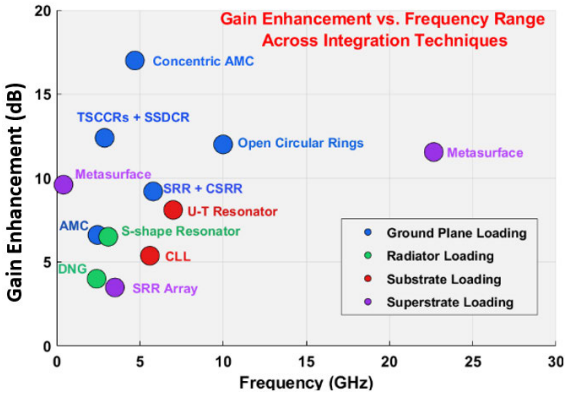

FIGURE 9. Gain enhancement across frequency ranges for various integration techniques as discussed above.

whereas Fig. 9 highlights the amount of gain enhancement at different frequencies across integration techniques as discussed above. Ground plane loading, particularly with AMC structures, delivers the highest gain enhancements, reaching up to 17.2 dB (Fig. 9), and is ideal for applications requiring strong directional radiation, although it often involves increased fabrication complexity. Superstrate loading, using metasurfaces or GRIN lenses, balances gain enhancement with broader bandwidths and frequency as shown in Fig. 9, making it well-suited for high-frequency applications like 5G or satellite communications. Radiator loading techniques, such as SRRs and SSDCRs typically result in narrower bandwidths, which limits their applicability for ultra-wideband systems. Substrate loading, while compact, faces challenges with efficiency due to potential substrate losses, though techniques like U-T shaped resonators embedded in substrates have shown significant performance improvements in specific cases. In regard to the impact on the overall profile of the antenna as seen in Table 1, ground plane loading, particularly with AMC-backed designs, can significantly increase size (>200%) due to additional unit cell arrays, while EBG-based ground planes exhibit moderate size growth. Radiator loading generally maintains a compact footprint (50% to 89.6%), but larger unit cell arrays slightly expand the structure. Substrate loading is appeared to be the space-efficient, with embedded unit cells minimizing external modifications and achieving up to 75% compactness. Superstrate loading, especially GRIN lenses and SIC-based layers, increases profile height, though metasurface-based designs offer low-profile alternatives.

Now that we have reviewed the primary techniques of metamaterial integration, the following section evaluates how these methods have been implemented in real antenna designs, analyzing their benefits, challenges, and observed gain improvements.

B. PERFORMANCE ANALYSIS OF METAMATERIAL-INTEGRATED ANTENNAS

Generally, we have considered three key approaches of using metamaterials in enhancing antenna gain which are [26]:

AQ:3 **TABLE 1. Comparative performance analysis of metamaterial integration methods.**

Integration Type	Metamaterial Structure	Frequency Range (GHz)	Gain Enhancement (dB)	Bandwidth Impact	Size Impact	Radiation Efficiency (%)
Ground plane Loading [27]	AMC with 2x2 array of hexagonal unit cells	2.45, 5.80	1.89 to 6.61 (2.45 GHz), 4.10 to 8.02 (5.80 GHz)	Bandwidths of 10.12% and 7.43% at respective frequencies	Size increased >200%	>87%; slightly reduced after AMC integration
Radiator Loading [11]	Array of 3x6 S-shape unit cells	3.1-3.88	6.5 (Increased by 1.8 dB)	Achieved 22.3% bandwidth	Array of unit cells increases the size 50%	Not mentioned
Radiator Loading [12]	Diagonal pattern DNG	2.4–2.484, 5.15–5.85	1.0 to 4.0 (at 2.5 GHz)	Bandwidths of 16.8% and 17.84% at respective frequencies	Size increased by 50%	Not mentioned
Radiator Loading [13]	Modified SRR	2.4–2.5, 8.01–8.5	3.63 (lower band), 1.00 (upper band)	16% increase in lower band, 6% increase in upper band	89.6% compact	Increased (not quantified)
Ground Plane Loading [21]	3x3 array of AMC with concentric ring and plus-shaped slot	4.7, 9.9	3 to 4.5 (minimum), 14 to 17 (maximum)	Wideband improvement	16mm airgap added	Increased but not satisfactory (not quantified)
Ground Plane Loading [16]	Four triangular shapes capacitive couples resonators (TSCCRs) and square shaped with diagonal cross-slot (SSDCS)	2.88–14.0	7.2 at 12.39 GHz	Ultrawideband (2.88GHz-14 GHz) achieved	Size not impacted	87%
Ground Plane Etching [20]	SRR and CSRR (2x5 array of unit cells)	5.8	9.2	Significant improvement (250MHz to 1.78GHz)	Size increased	73%
Substrate Loading [22]	Capacitive Loaded Loop (CLL) immersed in the substrate	5.6, 6.08	5.37 (reduced from 6.43)	Increased (7.7% to 10.86%). 620 MHz.	Minimal impact (embedded in substrate)	~90%
Substrate Loading [23]	U-T shaped resonator embedded into substrate	7.0	8.1 (increased by 18%)	Increased (from 330GHz to 500GHz)	75% compact	98%
Superstrate loading [28]	Metasurface loaded above a substrate integrated cavity (SIC) antenna	22.65-28.00	11.55 (increased by 2)	Broadened bandwidth by >50%	May increase profile due to height of the superstrate	>90%
Superstrate loading [29]	metasurface positioned above a circular path antenna as a superstrate.	0.412	9.6 (increased by 5)	Improved (not quantified)	Low profile maintained	Not mentioned
Ground plane loading [30]	A reflectro composed of open circular rings placed below the antenna array	10.0	12.0 (increased by 6)	Reduced (from 6016 to 1283)	Size increased due to increasing array elements of both antenna and the reflector	79.11% (increased by 10%)
Superstrate loading [31]	2x2 array of SRR unit cells (double layer)	3.5	3.48 (increased by >3)	Not mentioned	Size increased due to two layers of superstrates	Not mentioned

i) reduction of back radiation and maximization of reflection,
ii) controlling of surface wave propagation, and,
iii) maneuvering of EM wave with engineered refractive index.

For (i) and (ii), metasurfaces such as artificial magnetic conductors (AMC) and electromagnetic band-gap (EBG) structures are considered whereas metalenses have been investigated for (iii). As discussed in the earlier section, AMC/EBG is typically loaded as reflector/modified ground plane of an antenna whereas superstrates generally act as metalenses. This section explores the utilization of specific types of metamaterial loadings, including AMC, EBG, and metalenses, exclusively used for gain enhancement.

1) ANTENNAS WITH AMC AND EBG

AMCs and EBG structures are engineered to mimic the properties of ideal magnetic and electric conductors, respectively. Both of them usually comprised by periodic arrangement of several unit cells as shown in Fig. 10. AMCs stand out from natural materials by showing robust magnetic responses at certain microwave frequencies [32], and are known for their high-impedance surfaces, effective in reflecting and scattering electromagnetic waves [33]. A distinctive aspect of AMCs is their ability to reflect electromagnetic waves while preserving their phase, a metal sheets or perfect electric conductors (PECs) in antennas, which often necessitate a quarter-wavelength spacing to mitigate destructive interference [34]. The in-phase reflection by AMCs results in constructive interference, effectively enhancing antenna gain. AMCs can be placed nearer to the antenna, thereby enhancing radiation patterns, boosting efficiency, and allowing for smaller antenna sizes. The specific operational frequency and bandwidth of an AMC are determined by its structure, which typically involves periodic metallic patterns on a dielectric substrate [35], [36].

AMCs are particularly useful in low-profile antenna designs for reducing back radiation, thereby increasing forward gain [37], [38]. An AMC-based antenna is presented in [39] featuring a 2-D periodic pattern on top of a 1.6 mm thick FR4 slab that creates an impedance surface. The bottom side has a ground plane with an inductive aperture, modifying the reflection phase across frequencies and serving as an alternative to perfect electric conductors (PECs), reducing the antenna profile to approximately $\lambda/10$ of its wavelength. This antenna achieves a notable gain increase, with a peak gain of 9.7 dB at broadside, 6.2 dB higher than a standard antenna without AMC. In another study [40], an AMC surface with a defected dumbbell-shaped unit cell (2×2 array) (Fig. 11 (a)) effectively redirects out-of-phase radiation towards the main beam at the, enhancing gain up to 8.6 dB, an 85% increase compared to a standard monopole antenna. Fig. 11 (b) represents the zero-reflection phase by the AMC surface which maximizes the radiation at 2.4 GHz. The capacitive effect of the AMC structure also provides dual-band functionality (2.4 GHz and 3.9 GHz). Study [21] utilizes an AMC surface to diminish back radiation in a microstrip-line fed UWB antenna, achieving peak gain of 17.8 dB. A 3×3 array of dual-band AMC cells, each 15×15 mm in size, features a square patch with a concentric ring and a plus-shaped slot as depicted in Fig. 12 (a), resonating at 4.7 and 9.9 GHz. The study finds optimal performance with a 16 mm air gap between the UWB antenna and the AMC structure, leading to gain enhancement across the entire operational frequency range. Fig. 12 (b) illustrates the gain improvement using AMC compared to the original antenna's gain.

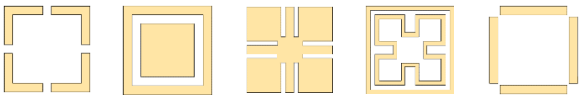

FIGURE 10. Unit cells of several AMCs/EBGs normally are backed by grounded dielectric slabs. Grey parts represent metallization [41].

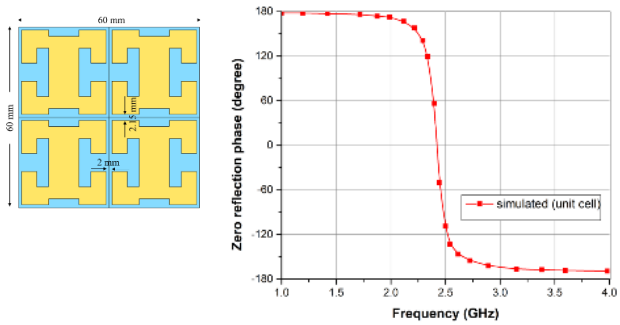

(a) (b)

FIGURE 11. (a) 2 × 2 array of defected dumbbell shaped AMC unit-cells (left) exhibits (b) Zero reflection phase at 2.4 GHz (right) to maximize radiation [40].

EBGs are characterized by their capacity to create a band gap that influences electromagnetic wave propagation, selectively blocking or reflecting waves at certain frequencies. Their primary role lies in mitigating surface waves and enhancing antenna performance, generally by minimizing mutual coupling and improving radiation characteristics [42]. EBG structures are primarily designed to develop frequency-selective surfaces, enabling specific manipulation of waves, while AMCs are utilized for their distinct reflection capabilities to enhance antenna performance. As illustrated in Fig. 13, an EBG surface functions as a ground plane for the antenna situated above it, maintaining a distance much less than half the wavelength ($d \ll \lambda_0/2$). This setup allows for the reflection of incident waves without any phase shift, thereby significantly improving the performance of the antenna [43]. By reducing surface waves, EBGs facilitate a greater proportion of power being radiated in the intended direction. This not only contributes to a more directive radiation pattern but also inherently increases the antenna's gain. In study [44], integrating a mushroom-type EBG structure into a modified microstrip patch antenna with a defected ground as shown

in Fig. 14 (a) notably improves its directivity and gain. This enhancement is particularly effective across the EBG's operational bandgap of 2.25 to 4.25 GHz as shown in Fig. 14 (b), due to its ability to suppress surface waves. Due to this distinct band gap property, EBG blocks electromagnetic wave propagation in specific frequency ranges. This feature creates high-impedance surfaces that reflect electromagnetic waves in phase, leading to constructive interference and thus, boosting radiated power [45].

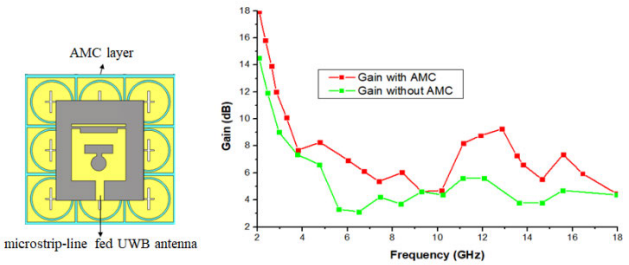

FIGURE 12. UWB antenna backed by AMC as proposed in [21]. (a) Top view, and (b) Gain comparison for the antenna with/without AMC.

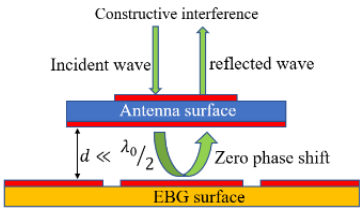

FIGURE 13. Working principle of an EBG surface. Zero phase shift results in constructive interference.

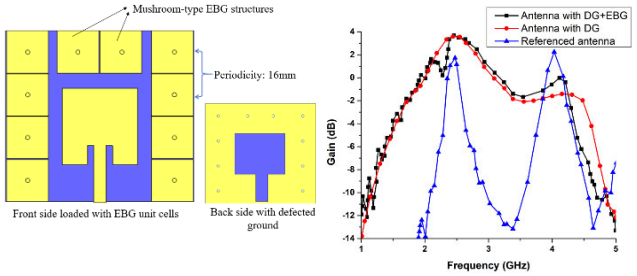

FIGURE 14. (a) Proposed antenna with mushroom like EBG structure (Yellow unit cells with vias), and (b) Gain at the operating bandgap region with and without EBG [44].

Table 2 and Table 3 provide overviews on design methods AMC and EBG structures with different antennas respectively to enhance gain across various frequencies and applications.

Additionally, Fig. 15 represents an overview of how both EBG and AMC contributes in gain improvement of antennas.

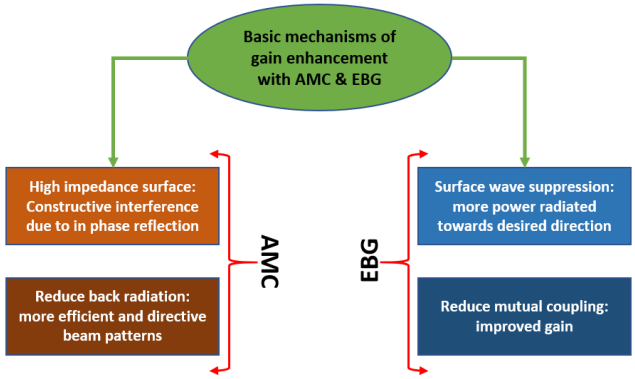

FIGURE 15. Techniques of how AMC and EBG contribute in gainenhancement [46], [47], [48], and [49].

2) ANTENNAS WITH METAMATERIAL LENSES

Metamaterial lenses (metalenses), renowned for their ability to focus radiation similarly to conventional lenses, offer distinct advantages over traditional dielectric lenses, as shown in [50] and [51]. These advantages include wideband operation and higher gain. Structurally, metalenses are typically categorized into two types: zero/near zero index and variable index lenses. Zero or near zero index lenses are considered to have fixed index property, whereas variable index lens features a spatially variable refractive index. Both types are discussed below:

a: ZERO INDEX AND NEAR ZERO INDEX LENSES

These types of lenses are constructed with Zero index materials (ZIM) or near zero index (NZI) materials exhibiting zero/near zero refractive index as the names suggest. Based on equation (1), their refractive index is directly attributed to their dielectric parameters. These zero or near zero values can take any value from zero axes regardless the regions/quadrants as shown in Fig. 1. These materials redirect electromagnetic waves perpendicular to their interface, following Snell's law, leading to gain improvement. This concentration of electromagnetic (EM) energy boosts antenna gain by making it more directive. The EM fields are evenly distributed but dynamically change, leading to a consistent electric field at the boundary. Consequently, ZIM/NZI functions like a phased aperture, typically integrated as a superstrate/layers of superstrates, focusing the radiation pattern and converting the antenna's curved phase front into a planar one, as depicted in the Fig. 16. This transformation enhances the antenna's directivity and gain [52].

ZIM and NZI superstrates are recognized as 2D lenses as shown in [53], [54], and [55], often involving single-layer substrates on the top of antennas. For instance, [53] introduces a single-layer 2D flat lens to increase the gain of a cylindrical antenna, maintaining a minimal distance of 0.4 λ_0 between the lens and the antenna, resulting in a 3.5 dB gain improvement. Similarly, in [54] a metasurface is placed 0.5λ above a 4-element MIMO antenna to enhance gain at

TABLE 2. AMC integrated antennas from literatures with enhanced gain.

Study	Design Methods	Frequency of Operations	Performance (gain)	How AMC Boosted Gain	Applications
[40]	Compact monopoles with defected stepped ground structures and defected dumbbell-shaped AMC unit cell.	2.4 GHz ISM, 3.9 GHz WiMAX	Gain increased by up to 8.6 dB (85% improvement over standard monopole)	AMC compensated out-of-phase radiation, increased gain through dual resonating band	ISM and WiMAX bands, suitable for close human interaction
[56]	Hexagonal UWB antenna with an AMC reflector.	Ultra-Wideband frequencies	Average gain improvement of 3.74 dB, peak gain of 5.5 dB, widened boresight gain band by ~1 GHz.	AMC reflector enhanced boresight and peak gain, expanded the effective gain band	Ultra-Wideband (UWB) applications, offering broader application range
[57]	Low-profiled microstrip design with an optimized AMC layer, optimization via genetic algorithm.	Frequencies suitable for 5G applications	Significant enhancement in peak gain (up to 9.8 dB) and front-to-back ratio, low side-lobe level (SLL).	Optimized AMC layer enhanced gain and improved front-to-back ratio	5G wireless systems, suitable for high-speed wireless communication
[58]	Coplanar waveguide (CPW) rectangular-ring antenna over a dual-band AMC structure.	2.45 GHz, 5.20 GHz	Gain increase of about 5 dB	AMC provided directional properties and gain improvement at dual frequencies.	Versatile for various wireless applications, focusing on dual-band operation
[59]	Antenna made using textile materials over an AMC, suitable for wearable technology.	2.4 GHz, 5.8 GHz	Realized gain increase of 4 dB, better human body isolation	AMC improved performance with better gain and human body isolation	WLAN applications, particularly in wearable technology

TABLE 3. EBG integrated antennas from literatures with enhanced gain.

Study	Design Methods	Frequency of Operations	Performance (gain)	How EBG Enhanced Gain	Applications
[43]	EBG structure with four spiral-shaped radiators are combined with centre element (0.03 λ0 × 0.03 λ0)	2.4 GHz	Increased gain by 1.7 dB	EBG provided high impedance surface for in-phase reflection, boosting gain	Microwave components
[44]	Mashroom type EBG structure on the top of substrate of an microstrip patch antenna. The antenna is modified with DG and EBG.	Antenna for ISM band operation. EBG for a bandgap of 2.25-4.25GHz	3.84 dB	Surface wave suppression and band gap creation	ISM band (monostatic and bistatic RCS in military and stealth platform for lower detectable objects)
[60]	A rectangular microstrip patch antenna with a mushroom-like EBG structure and with a novel triple side-slotted EBG (TSSEBG) (52mm X 50mm)	6 GHz	High gain (maximum 10.16 dB) and directivity with efficient beam steering.	EBG provided band-stop and band-pass properties, and suppressed surface waves, enhancing gain	Wireless, satellite applications
[61]	Z-shape EBG structure in a phased antenna array (2X2) (no dimension mentioned)	2.4GHz	9.2 dB (maximum) among all 9 beam scanning states	Not specified	Locating, tracking, and landing UAVs - using antennas and antenna arrays (AR)
[62]	A patch antenna modified with a polarization-dependent metamaterial surface made of blocks of slotted EBG structures. These structures are arranged in a chessboard configuration for scattering cancellation.	2.85 to 3.95 GHz	Increased gain by more than 2.5 dB	By studying and controlling induced current on the EBG as a novel mechanism for gain enhancement	Stealth platforms and modern wireless communication devices

approximately 26GHz. The metasurface comprises a 9 × 6 array of circular split rings with extracted permittivity and permeability values of the unit cell as shown in Fig. 17. Study [63] employs a 2D ZIM lens in a different way on the aperture of the radiator (Fig. 18) rather than as a superstrate. This lens is a compound optical lens (COL), combination of a plano-convex lens and a double convex lens, which is not only able to convert spherical wave into a planar one, but also it can focus the converted wave into a direction with a very narrow beam of as low as 11.2°. Extremely narrow beam resulted both gain and directivity enhancement of an antipodal Vivaldi antenna very effectively. The dual lens action of the loaded metamaterial at the aperture of the antenna is demonstrated in the Fig. 18. Compared to single-layer 2D ZIM/NZI, adding

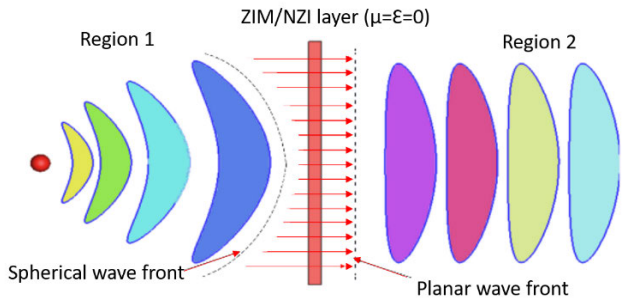

FIGURE 16. Conversion of curved phase (region 1) into planar phase (region 2) through ZIM/NZI layer.

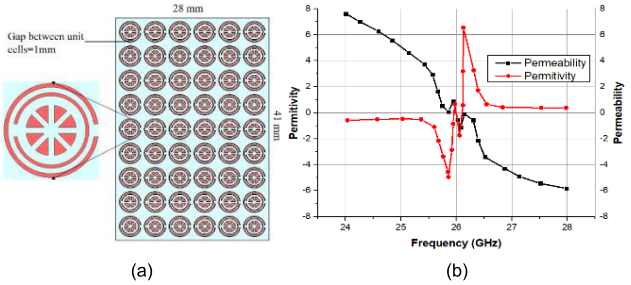

FIGURE 17. The array of circular split rings used as a metasurface for a MIMO system proposed in [54]. (a) the unit cells and array. (b) extracted parameters of the unit cells at 26 GHz.

multiple superstrate layers as bulk metamaterial enhances gain further. For example, [64] employs a double-layer ZIM lens, made from flower-shaped unit cells, to boost the gain of a conventional microstrip patch antenna for the Ku band, increasing boresight gain by over 150%. In [52], a nested Schurig SRR superstrate functions as a dual-band ZIM, transforming a classical monopole into a high- gain dual-band antenna. An 8 × 8 array of these unit cells is stacked and placed above the monopole antenna for further gain enhancement by adding more ZIM layers [52], as demonstrated in Fig. 19. Similarly, in [65], a significant gain enhancement is observed by adding layers of superstrates where a 7 × 7 array of unit cells, developed by appropriately adding metal strips, is placed on a patch antenna for WiMAX applications. Two layers of NZI as superstrate result in a peak gain of 8.26 dB with an increased half-power beam width of 52 degrees. As the research continues, numerous approaches for gain enhancement using NZI and ZIM as superstrates are applied to different antenna types, such as circular patched antennas [66], a tapered log periodic dipole antenna for multiband operation [67], a miniaturized patch antenna [68], and more. However, the height of the superstrate remains a constraint in considering the antenna's profile, and meticulous selection of this parameter is necessary to balance between size and the gain of an antenna.

b: VARIABLE INDEX LENSES

The prevalent concept in utilizing 2D or bulk ZIM/NZI lenses, as covered in the previous section and various

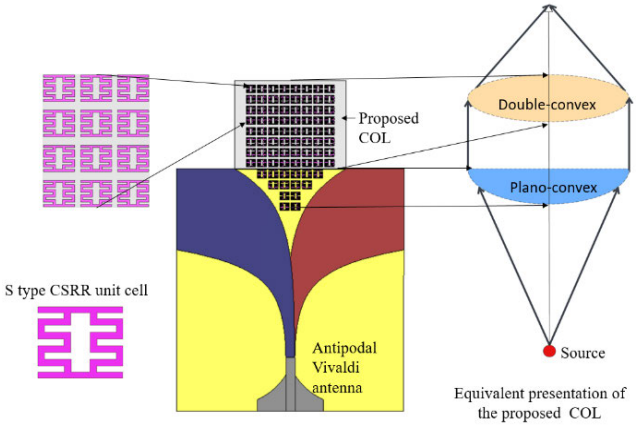

FIGURE 18. The Vivaldi antenna (in the middle) with compound lens at the flare end of the antenna. CSRR used in the lens is shown at the left. The simple equivalent presentation of the compound lens is at the right [63].

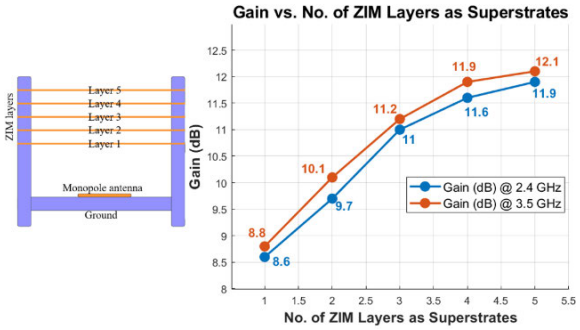

FIGURE 19. The corresponding gain enhancement of a classical planar monopole antenna (left) for increasing the number of ZIM superstrate layers [52]. Gain improves as number of layers increases from 1 to 5 at both frequencies (right).

literatures, involves positioning them as single (2D structure) or multiple layers (bulk structure) near or directly on the radiators. These lenses typically operate with a single refractive index (either zero or near-zero) across the desired frequency range. On the other hand, varying indices by changing shape, size, orientation and other geometric patterns of the unit cells provides a more comprehensive way to design antenna with high gain, beam manipulation and directivity features. A specific example is given in [69], where a lens is designed with unit cells of varying shapes, geometries, and orientations to enable beam manipulation and gain enhancement. The lens, with dimensions of 50.4 mm x 50.4 mm, features a 28 × 28 array of unit cells, each differing in size. These cells are engineered to produce discrete phase delays in the electromagnetic waves originating from a 1.6 dB dipole feed antenna, attributable to their spatially variable refractive index. This arrangement efficiently focuses the waves emitted from a linear feed array into collimated beams, achieving a peak gain of 14 dB at 28 GHz. Importantly, the gain can be further increased without enlarging the lens's aperture at higher frequencies, as the unit cells correspond to the

wavelength of the EM wave. The study also reveals that the optimal position for the antenna to attain maximum gain is at the lens's focal point. Deviating from this position leads to a decrease in gain due to phase offset which illustrates the setup and the corresponding gain response [69].

Amongst variable index lenses, gradient index (GRIN) lenses, which function through the alteration of geometric parameters and shapes for beam manipulation, are currently under thorough investigation for their potential in enhancing antenna gain. The GRIN lens's ability to gradually vary its refractive index enables it to operate similarly to a conventional optical lens, shaping and directing beams effectively. Within the realm of GRIN lenses, the Luneburg lens and Maxwell's Fish eye lens stand out as particularly promising for improving both gain and directivity [8]. The specific refractive index (n) distributions for the Luneburg lens and Maxwell's Fish eye lens are given by [70],

$$n(r) = \sqrt{\epsilon_r} = \sqrt{2 - (\frac{r}{R})^2}, \quad 0 \le r \le R \tag{5}$$

and

$$n(r) = \sqrt{\epsilon_r} = \sqrt{2 - \frac{n_0}{1 + (\frac{r}{R})^2}}, \quad 0 \le r \le R \tag{6}$$

respectively. Here ϵ_r is relative permittivity, R is the radius of lens, and r denotes the distance between center and any points. The Luneburg lens is characterized by a radially symmetric refractive index that decreases from the center to the periphery, enabling it to focus beams arriving from any direction on its surface to a diametrically opposite point. On the other hand, Maxwell's Fish-Eye lens, which is based on a specific refractive index formula, theoretically maps each point on its surface to another surface point. However, this remains largely a theoretical concept with limited practical implementations [55]. GRIN lenses function in the non-resonant regions of their unit cells, overcoming the narrow bandwidth and high transmission loss issues typically associated with ZIM/NZI materials, thereby facilitating enhanced broadband gain. A notable development in this field is presented in [71], which introduces a ten-layer 3-D Luneburg lens (Fig. 20) designed for C band frequencies. This lens is constructed using vertical dielectric slabs combined with metamaterials featuring a non-bianisotropic SRR (NB-SRR) to achieve a variable refractive index. Positioning a small dipole at the lens's focal point elevates its gain from 1.6 dB to 15.2 dB at 7 GHz, making its performance comparable to a conventional parabolic antenna. Such a lens offers significant gain enhancement for linear antennas, particularly those with minimal polarization angle or those that are circularly or elliptically polarized.

Another 10-layered GRIN lens is proposed in [72] which conducts extraction of parameters like permittivity, permeability, and refractive index through Kramers–Kronig relations [73] based on the geometry and shapes of the unit cells for a specified frequency range. The varying parameters of the unit cells are shown in Fig. 21(a), and unit cells are strategically distributed within the lens to ensure consistent performance across lower and higher frequencies. The study achieves a remarkable peak gain of 20.55 dB at an operating bandwidth of 0.84-11.5 GHz for an Ultra-Wide Band (UWB) antipodal tapered slot antenna (Fig. 21 (b)), achieved by positioning six lenses in front of it, as depicted in Fig. 21 (c). Fig. 21 (d) shows corresponding gain improvement after integrating GRIN lens. Study [70] investigates ways to enhance the gain of a standard monopole antenna by utilizing seven parallel-line metamaterial GRIN lenses. This approach is similar to the techniques outlined in study [67]. These lenses exhibit a refractive index ranging from 1.1 to 1.67, correlating with the unit cell length across the frequency spectrum of 2-11 GHz. This configuration results in a maximum gain 50% higher than the basic monopole antenna alone. Further, [74] proposes a three-layer GRIN lens design, with the core layer flanked by two impedance matching layers. This study achieves a wider refractive index range (1.75-5.5) over the length of the core layer's unit cells. Additionally, the symmetric structure of the lens allows for desirable gradient indexes in two orthogonal polarizations with an isolation of 30 dB. Table 4 provides an overview of recent literature, showcasing different lenses, their structures, and performances.

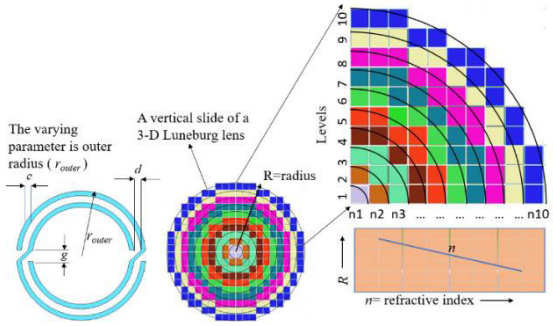

FIGURE 20. NB-SRRs as the unit cell with varying parameter to vary refractive index (left), Sectional view of ten-layered Luneburg lens (middle) theoretically established in [71]where different colors represent different values of refractive index specific to a single layer/level as shown by numbers (right). Index decreases as the radius of the lens increases.

IV. DISCUSSION AND FUTURE CHALLENGES

AMCs and EBGs, when used as modified ground planes or reflectors, significantly improve radiation efficiency by suppressing surface waves and creating constructive interference. AMCs, characterized by high-impedance surfaces, effectively convert omnidirectional radiation into directional patterns, making them particularly suitable for low-profile antenna applications. EBG structures, on the other hand, improve front-to-back ratio and reduce mutual coupling in array configurations.

Metamaterial lenses, such as graded-index (GRIN) lenses, zero-index (ZIM), and near-zero-index (NZI) superstrates, manipulate electromagnetic wave propagation to enhance gain. GRIN lenses, with a continuous refractive index

TABLE 4. Metamaterial lenses from literatures showing designs, types and performances.

Study	Lens dimension	Distance from antenna	Performance	Application	antenna	Lens type
[53]	$1.9\lambda_0 \times 1.9\lambda_0 \times 0.05\lambda_0$ (7X7 array)	0.4 λ_0	2-3.5 dB gain enhancement between 1.3 and 1.45 GHz	Variety of antenna applications	Cylindrical antenna	Single flat lens
[54]	28mm x 41mm (9X6 array of CSR)	0.5 λ_0	Peak gain 10.27 dB	5G mm-Wave (24.55-26.5GHz)	4-element MIMO	Single flat lens
[64]	2X3 array Flower shaped DNG unit cells (15x10x1.55)	5mm between two lens layers, 10 mm between the first lens and the antenna	Peak gain 4.58 dB at 12 GHz	Ku band	A conventional microstrip patch antenna	Double flat lens
[63]	S type CSRR. Unit cell: 3.1mm X 4.6mm	At the aperture	Maximum gain enhancement 5 dB Min HPBW 11.2°	6, 9 and 12 GHz	Antipodal vivaldi	Compound optical lens
[69]	28x28 array of metallic unit cell on a substrate of 50.4 mm x 50.4 mm	2cm (2 λ_0)	Maximum gain 14 dB	28 GHz	A dipole feed antenna	Large aperture lens
[72]	Radius: 114 mm Thickness: 20.71mm	100 mm (at focal point)	Maximum gain: 20.55 dB	0.85-11 GHz	Ultrawideband Antipodal Tapered Slot Antenna	GRIN lens
[75]	84mm x 60mm	23mm	Maximum gain: 9.8 dB	2-11GHz	Basic Monopole	Parallel-line GRIN lens

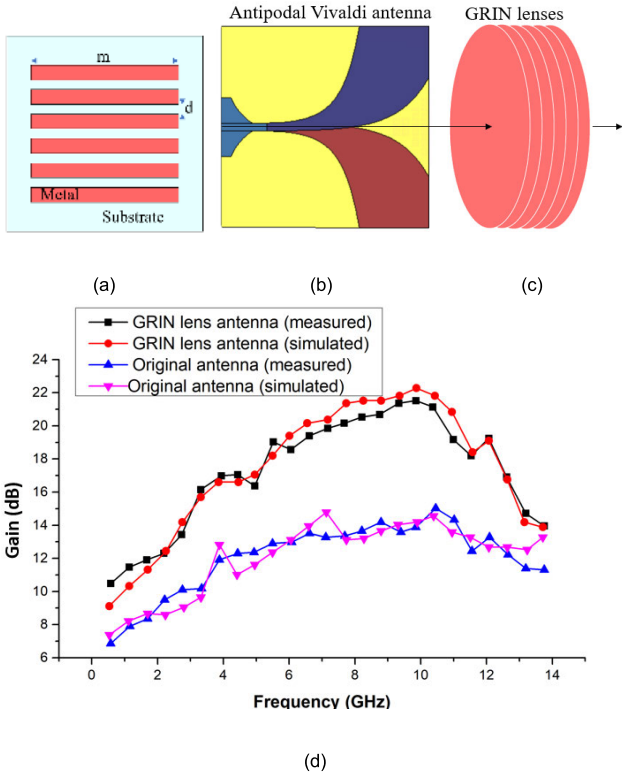

FIGURE 21. 10-layered GRIN lens to enhance gain of an antipodal Vivaldi antenna. (a)The unit cell with varying parameters (*m* and *d*). (b) antenna. (c) GRIN lens with designed unit cells in front of the antenna [72]. (d) the gain response of the antenna with and without lens.

TABLE 5. Challenges and future research directions.

Category	Challenges/Limitations	Insights/Future Directions
Size vs. Gain Trade-Off	Gain enhancement often increases antenna size/profile, particularly with superstrates and metasurface lenses.	Investigate compact metamaterial designs like GRIN lenses on radiators.
Unit Cell Design	Increasing unit cells improves gain but hinders miniaturization, affecting compact antenna designs.	Optimize unit cell geometries to balance size and performance.
GRIN Lenses	Complex designs require multi-layer refractive indices, making fabrication and integration challenging.	Develop planar or low-profile GRIN lenses and explore 3D printing for fabrication.
Fabrication Issues	3D GRIN lenses remain largely theoretical, with most studies using simplified 2D models.	Advance fabrication techniques, such as additive manufacturing technique, for practical implementation and optimize materials.
Parameter Extraction	Standardized methods for extracting permittivity, permeability, and refractive index remain unclear.	Establish design guidelines for SRR, CSRR, and other metamaterial unit cells.
Antenna Type Dependency	Most metamaterial integration focuses on planar antennas, limiting broader applicability.	Extend research to non-planar, conformal, and wearable antennas for versatile designs.

gradient, offer superior beamforming capabilities while maintaining consistent gain across wide scanning angles, an advantage over traditional phased arrays that suffer from gain reduction at extreme steering angles. ZIM/NZI superstrates, particularly in Fabry-Perot configurations, concentrate electromagnetic energy by transforming a curved phase front into a planar one, maximizing constructive interference. These are especially beneficial for antennas with existing directive patterns, enhancing their gain without altering the primary radiation characteristics.

Among these techniques, GRIN lenses exhibit the most consistent performance, as their non-resonant metamaterial cells allow broadband operation with minimal loss. Unlike AMC-based solutions, which are optimal for enhancing directional radiation in low-profile designs, GRIN lenses facilitate continuous beam manipulation with high efficiency. While metamaterial-assisted gain enhancement has shown significant progress, challenges remain in optimizing fabrication techniques, minimizing losses in practical implementations, and extending performance across broader frequency ranges. Based on the analysis and investigation, followings challenges could be addressed and based on which future research directions can be suggested (See Table 5).

V. CONCLUSION

This review underscores the transformative impact of metamaterials in antenna design for enhancing gain. It highlights the theoretical background of major types of metamaterials, their characteristics, and integration in the antenna systems for enhancing gain. A comprehensive analysis between different integration techniques in terms of their performances has been explored. Additionally, there is a significant investigation on antennas integrated with major types of metamaterials. Despite metamaterial's advancements, the review also acknowledges the challenges and complexities involved in integrating metamaterials with antenna systems. The design and fabrication of metamaterial-equipped antennas require careful consideration of factors like the existing radiation pattern of the antenna, desired directionality, and bandwidth requirements. The integration process often demands a blend of different metamaterials to achieve optimal performance, adding to the complexity of antenna design.

REFERENCES

[1] C. C. M. Chryssomallis, "Radiation patterns," in *Encyclopedia of RF and Microwave Engineering*, K. Cheng, Ed., Hoboken, NJ, USA: Wiley, 2024.

[2] M. P. Jyothi, T. P. Surekha, and A. J. S. Kumar, "Innovative designs and performance evaluation of super wideband MIMO antennas: A survey," *Nondestruct. Test. Eval.*, vol. 12, pp. 1–32, Jan. 2025.

[3] W. Zhu, Q. Song, L. Yan, W. Zhang, P. Wu, L. K. Chin, H. Cai, D. P. Tsai, Z. X. Shen, T. W. Deng, S. K. Ting, Y. Gu, G. Q. Lo, D. L. Kwong, Z. C. Yang, R. Huang, A. Liu, and N. Zheludev, "A flat lens with tunable phase gradient by using random access reconfigurable metamaterial," *Adv. Mater.*, vol. 27, no. 32, pp. 4739–4743, Aug. 2015.

[4] C. Milias, R. B. Andersen, P. I. Lazaridis, Z. D. Zaharis, B. Muhammad, J. T. B. Kristensen, A. Mihovska, and D. D. S. Hermansen, "Metamaterial-inspired antennas: A review of the state of the art and future design challenges," *IEEE Access*, vol. 9, pp. 89846–89865, 2021.

[5] H. Fernández-Álvarez, M. E. de Cos Gómez, and F. L.-H. Andrés, "The challenge of modeling grounded metasurfaces: A new approach to obtain their constitutive parameters," *Appl. Phys. A*, vol. 128, no. 11, pp. 1–8, 2022.

[6] D. Panchal and V. A. Rana, "Metamaterial absorbers: Materials, properties, and performances," in *Handbook of Nano-Metamaterials* (Metamaterials Science and Technology), vol. 1. Singapore: Springer, 2024, pp. 1–47.

[7] N. Ullah, L. Lee, M. S. Islam, and M. T. Islam, "A compact, polarization-insensitive, double negative (DNG) perfect metamaterial absorber for electromagnetic energy harvesting applications," in *Proc. 2nd Asia Conf. Electron. Eng. (ACEE)*, Singapore, Apr. 2024, pp. 36–39.

[8] F. Tariq, M. R. A. Khandaker, K.-K. Wong, M. A. Imran, M. Bennis, and M. Debbah, "A speculative study on 6G," *IEEE Wireless Commun.*, vol. 27, no. 4, pp. 118–125, Aug. 2020.

[9] S. K. Ibrahim, S. S. Al-Bawri, M. J. Singh, H. H. Ibrahim, M. T. Islam, M. S. Islam, W. M. Abdulkawi, and A.-F.-A. Sheta, "Compact metamaterial-based single/double-negative/near-zero index resonator for 5G sub-6 GHz wireless applications," *Sci. Rep.*, vol. 14, no. 1, pp. 23–36, Jun. 2024.

[10] J. Zhang, S. Yan, and G. A. E. Vandenbosch, "Metamaterial-inspired dual-band frequency-reconfigurable antenna with pattern diversity," *Electron. Lett.*, vol. 55, no. 10, pp. 573–574, May 2019.

[11] R. Sahoo and D. Vakula, "Gain enhancement of conformal wideband antenna with parasitic elements and low index metamaterial for WiMAX application," *Proc. AEU-Int. J. Electron. Commun.*, vol. 105, pp. 24–35, Mar. 2019.

[12] S. Roy and U. Chakraborty, "Gain enhancement of a dual-band WLAN microstrip antenna loaded with diagonal pattern metamaterials," *IET Commun.*, vol. 12, no. 12, pp. 1448–1453, Jul. 2018.

[13] S. Roy and U. Chakraborty, "Metamaterial-embedded dual wideband microstrip antenna for 2.4 GHz WLAN and 8.2 GHz ITU band applications," *Waves Random Complex Media*, vol. 30, no. 2, pp. 193–207, Apr. 2020.

[14] A. Mehdipour, T. A. Denidni, and A.-R. Sebak, "Multi-band miniaturized antenna loaded by ZOR and CSRR metamaterial structures with monopolar radiation pattern," *IEEE Trans. Antennas Propag.*, vol. 62, no. 2, pp. 555–562, Feb. 2014.

[15] N. Amani, M. Kamyab, A. Jafargholi, A. Hosseinbeig, and J. S. Meiguni, "Compact tri-band metamaterial-inspired antenna based on CRLH resonant structures," *Electron. Lett.*, vol. 50, no. 12, pp. 847–848, May 2014.

[16] K. Neeshu and A. K. Tiwary, "Metamaterial loaded antenna with improved efficiency and gain for wideband application," *IETE J. Res.*, vol. 69, no. 3, pp. 1309–1316, Apr. 2023.

[17] A. D. Tadesse, O. P. Acharya, and S. Sahu, "Application of metamaterials for performance enhancement of planar antennas: A review," *Int. J. RF Microw. Comput.-Aided Eng.*, vol. 30, no. 5, May 2020, Art. no. e22154.

[18] M. Kashanianfard and K. Sarabandi, "Metamaterial inspired optically transparent band-selective ground planes for antenna applications," *IEEE Trans. Antennas Propag.*, vol. 61, no. 9, pp. 4624–4631, Sep. 2013.

[19] H. Malekpoor and S. Jam, "Improved radiation performance of low profile printed slot antenna using wideband planar AMC surface," *IEEE Trans. Antennas Propag.*, vol. 64, no. 11, pp. 4626–4638, Nov. 2016.

[20] N. L. Nguyen and Van Yem Vu, "Gain enhancement for MIMO antenna using metamaterial structure," *Int. J. Microw. Wireless Technol.*, vol. 11, no. 8, pp. 851–862, Oct. 2019.

[21] D. Negi, K. Kaur, A. Bansal, B. Dua, N. Singh, and S. Dhyani, "Back radiation reduction in a UWB antenna using metamaterial surface for wireless communication devices," in *Proc. 2nd, Ed., IEEE Delhi Sect. Flagship Conf. (DELCON)*, Rajputra, India, Feb. 2023, pp. 1–5.

[22] A. M. Lima, N. H. O. Cunha, and J. P. D. Silva, "Effect of metamaterial cells array on a microstrip patch antenna design," *J. Microw., Optoelectron. Electromagn. Appl.*, vol. 19, no. 3, pp. 327–342, Sep. 2020.

[23] P. Dawar, N. S. Raghava, and A. De, "High gain, directive and miniaturized metamaterial C-band antenna," *Cogent Phys.*, vol. 3, no. 1, pp. 1–12, 2016.

[24] S. Luo, Y. Zhang, P. Mei, G. F. Pedersen, and S. Zhang, "Decoupling for millimeter-wave array antennas using near-field shrinking dielectric superstrate," *IEEE Open J. Antennas Propag.*, vol. 4, pp. 1187–1194, 2023.

[25] R. Mark, N. Rajak, K. Mandal, and S. Das, "Metamaterial based superstrate towards the isolation and gain enhancement of MIMO antenna for WLAN application," *AEU-Int. J. Electron. Commun.*, vol. 100, pp. 144–152, Feb. 2019.

[26] Y. Zhao, K. Yu, and Y. Li, "A high gain patch antenna using negative permeability metamaterial structures," in *Proc. Prog. Electromagn. Res. Symp.-Fall (PIERS-FALL)*, Singapore, 2017, pp. 119–123.

[27] U. Ali, S. Ullah, A. Basir, S. Yan, H. Ren, B. Kamal, and L. Matekovits, "Design and performance investigation of metamaterial-inspired dual band antenna for WBAN applications," *PLoS ONE*, vol. 19, no. 8, Aug. 2024, Art. no. e0306737.

[28] Y. Yan, Z. Ma, W. Hao, H. Zhai, N. Wang, and C. Zhu, "High-gain substrate integrated cavity circularly-polarized antenna loaded with metasurface," in *Proc. Int. Appl. Comput. Electromagn. Soc. Symp. (ACES-China)*, Xi'an, China, Aug. 2024, pp. 1–2.

[29] C. Scarselli, E. Giusti, D. Brizi, and A. Monorchio, "Gain enhancement of a dual circularly polarized patch antenna based on electromagnetic metasurfaces," in *Proc. IEEE Int. Symp. Antennas Propag. INC/USNC-URSI Radio Sci. Meeting (AP-S/INC-USNC-URSI)*, Florence, Italy, Jul. 2024, pp. 315–316.

[30] S. H. Ali and A. K. Jassim, "Single layer metamaterial superstrate for gain enhancement of a microstrip antenna array," *Diyala J. Eng. Sci.*, vol. 17, no. 2, pp. 144–172, Jun. 2024.

[31] M. A. Saleim, N. A. Murad, N. A. Samsuri, T. T. Estu, and L. O. Nur, "Gain enhancement of fractal antenna using metamaterial," in *Proc. IEEE Int. Conf. Adv. Telecommun. Netw. Technol. (ATNT)*, Sep. 2024, pp. 1–4.

[32] J. B. Pendry, A. J. Holden, W. J. Stewart, and I. Youngs, "Extremely low frequency plasmons in metallic mesostructures," *Phys. Rev. Lett.*, vol. 76, no. 25, pp. 4773–4776, Jun. 1996.

[33] J. B. Pendry, A. J. Holden, D. J. Robbins, and W. J. Stewart, "Magnetism from conductors and enhanced nonlinear phenomena," *IEEE Trans. Microw. Theory Techn.*, vol. 47, no. 11, pp. 2075–2084, Nov. 1999.

[34] D. Schurig, J. J. Mock, B. J. Justice, S. A. Cummer, J. B. Pendry, A. F. Starr, and D. R. Smith, "Metamaterial electromagnetic cloak at microwave frequencies," *Science*, vol. 314, no. 5801, pp. 977–980, Nov. 2006.

[35] H. Chen, L. Ran, J. Huangfu, X. Zhang, K. Chen, T. M. Grzegorczyk, and J. A. Kong, "Negative refraction of a combined double S-shaped metamaterial," *Appl. Phys. Lett.*, vol. 86, no. 15, pp. 1–8, Apr. 2005.

[36] D. Sievenpiper, L. Zhang, R. F. J. Broas, N. G. Alexopolous, and E. Yablonovitch, "High-impedance electromagnetic surfaces with a forbidden frequency band," *IEEE Trans. Microw. Theory Techn.*, vol. 47, no. 11, pp. 2059–2074, Dec. 1999.

[37] T. U. Pathan and B. Kakde, "A compact circular polarized MIMO fabric antenna with AMC backing for WBAN applications," *Adv. Electromagn.*, vol. 11, no. 3, pp. 26–33, Aug. 2022.

[38] L. Han, K. Chai, G. Han, X. Chen, and W. Zhang, "Compact broadband circularly polarized slot antenna with artificial magnetic conductor reflector," *Int. J. RF Microw. Comput.-Aided Eng.*, vol. 32, no. 12, pp. 1–7 2022.

[39] M. N. Santhosh, T. A. Mehir, J. J. Solomon, and S. Bashyam, "Design and analysis of artificial magnetic conductor (AMC) for 5G communications," in *Proc. 4th Int. Conf. Emerg. Technol. (INCET)*, Belgaum, India, May 2023, pp. 1–6.

[40] B. Hazarika, B. Basu, and A. Nandi, "Design of antennas using artificial magnetic conductor layer to improve gain, flexibility, and specific absorption rate," *Microw. Opt. Technol. Lett.*, vol. 62, no. 12, pp. 3928–3935, Dec. 2020.

[41] A. Foroozesh and L. Shafai, "Investigation into the application of artificial magnetic conductors to bandwidth broadening, gain enhancement and beam shaping of low profile and conventional monopole antennas," *IEEE Trans. Antennas Propag.*, vol. 59, no. 1, pp. 4–20, Jan. 2011.

[42] M. Alibakhshikenari, B. S. Virdee, C. H. See, R. A. Abd-Alhameed, F. Falcone, and E. Limiti, "Surface wave reduction in antenna arrays using metasurface inclusion for MIMO and SAR systems," *Radio Sci.*, vol. 54, no. 11, pp. 1067–1075, Nov. 2019.

[43] C. Mohan, S. E. Florence, R. V. Samsingh, and N. Ahmed, "Design of a highly miniaturized novel electromagnetic bandgap (EBG) material for performance improvement in microwave components," *IOP Conf. Ser., Mater. Sci. Eng.*, vol. 1070, no. 1, Feb. 2021, Art. no. 012084.

[44] D. Singh, A. Thakur, and V. M. Srivastava, "Miniaturization and gain enhancement of microstrip patch antenna using defected ground with EBG," *J. Commun.*, vol. 13, no. 12, pp. 730–736, Jun. 2018.

[45] R. Ohashi, T. Tanaka, S. Yamamoto, M. Takikawa, and Y. Inasawa, "A design of multi-band mushroom-type EBG structure with multi-layer configuration," *IEICE Commun. Exp.*, vol. 10, no. 9, pp. 115–116, 2021.

[46] K. Kanjanasit, P. Osklang, T. Jariyanorawiss, A. Boonpoonga, and C. Phongcharoenpanich, "Artificial magnetic conductor as planar antenna for 5G evolution," *Comput., Mater. Continua*, vol. 74, no. 1, pp. 503–522, 2023.

[47] D. Gebeşoğlu, M. Kuloğlu, A. O. Ertay, and S. Şimşek, "Low-profile closed cavity backed spiral antennas with circular AMC reflector for V/UHF bands," *AEU-Int. J. Electron. Commun.*, vol. 170, pp. 1–10, May 2023.

[48] M. A. B. Abdullah, M. K. A. Rahim, N. A. Samsuri, M. Fairus, M. K. H. Ismail, and H. A. Majid, "On human body transmission wearable diamond dipole antennas above engineered jackets," *Indonesian J. Electr. Eng. Comput. Sci.*, vol. 22, no. 3, pp. 1513–1519, Jun. 2021.

[49] C. D. Bui, A. Desai, T. T. K. Nguyen, and T. K. Nguyen, "Fully transparent metamaterial amc backed CPW fed monopole antenna for IoT applications," *Vietnam J. Sci. Technol.*, vol. 59, no. 5, pp. 623–633, Oct. 2021.

[50] F. Ansarudin, T. A. Rahman, and Y. Yamada, "Design of dielectric lens antenna for 5G mobile base station," in *Proc. Int. Symp. Antennas Propag. (ISAP)*, Busan, South Korea, Oct. 2018, pp. 1–2.

[51] K. Konstantinidis, A. P. Feresidis, C. C. Constantinou, E. Hoare, M. Gashinova, M. J. Lancaster, and P. Gardner, "Low-THz dielectric lens antenna with integrated waveguide feed," *IEEE Trans. THz Sci. Technol.*, vol. 7, no. 5, pp. 572–581, Sep. 2017.

[52] Z. Haider, M. U. Khan, and H. M. Cheema, "A dual-band zero-index metamaterial superstrate for concurrent antenna gain enhancement at 2.4 and 3.5 GHz," *IETE J. Res.*, vol. 68, no. 4, pp. 2898–2908, Jul. 2022.

[53] M. Luo, X. Sang, J. Tan, and J. Chen, "A novel miniaturized metamaterial lens antenna," *Int. J. RF Microw. Comput.-Aided Eng.*, vol. 30, no. 7, pp. 1–8, 2020.

[54] S. Tariq, S. I. Naqvi, N. Hussain, and Y. Amin, "A metasurface-based MIMO antenna for 5G millimeter-wave applications," *IEEE Access*, vol. 9, pp. 51805–51817, 2021.

[55] W. Tang, J. Chen, and T. J. Cui, "Metamaterial lenses and their applications at microwave frequencies," *Adv. Photon. Res.*, vol. 2, no. 10, Oct. 2021, Art. no. 2100001.

[56] A. Joshi and R. Singhal, "Gain enhancement in probe-fed hexagonal ultra wideband antenna using AMC reflector," *J. Electromagn. Waves Appl.*, vol. 33, no. 9, pp. 1185–1196, Jun. 2019.

[57] A. Hocini, N. Melouki, and T. A. Denidni, "Modeling and simulation of an antenna with optimized AMC reflecting layer for gain and front-to-back ratio enhancement for 5G applications," *J. Phys., Conf. Ser.*, vol. 1492, no. 1, Apr. 2020, Art. no. 012006.

[58] F. Mouhouche, A. Azrar, M. Dehmas, and K. Djafer, "Gain enhancement of monopole antenna using AMC surface," *Adv. Electromagn.*, vol. 7, no. 3, pp. 69–74, Aug. 2018.

[59] A. Mersani, L. Osman, and J.-M. Ribero, "Improved radiation performance of textile antenna using AMC surface," in *Proc. 15th Int. Multi-Conf. Syst., Signals Devices (SSD)*, Yasmine Hammamet, Tunisia, Mar. 2018, pp. 627–631.

[60] M. K. Abdulhameed, M. S. B. M. Isa, Z. Zakaria, I. M. Ibrahim, M. K. Mohsen, M. L. Attiah, and A. M. Dinar, "Radiation control of microstrip patch antenna by using electromagnetic band gap," *AEU-Int. J. Electron. Commun.*, vol. 110, Oct. 2019, Art. no. 152835.

[61] I. Nachev and I. G. Iliev, "Z-shape EBG structure improving the phased antenna array radiation pattern with autonomous aerial vehicle navigation application," in *Proc. 30th Nat. Conf. Int. Participation (TELECOM)*, Sofia, Bulgeria, Oct. 2022, pp. 1–4.

[62] Z.-J. Han, W. Song, and X.-Q. Sheng, "Gain enhancement and RCS reduction for patch antenna by using polarization-dependent EBG surface," *IEEE Antennas Wireless Propag. Lett.*, vol. 16, pp. 1631–1634, 2017.

[63] H. Cheng, L. Hua, Y. Wang, H. Yang, and T. Lu, "Design of high gain Vivaldi antenna with a compound optical lens inspired by metamaterials," *Int. J. RF Microw. Comput.-Aided Eng.*, vol. 31, no. 4, Apr. 2021, Art. no. e22570.

[64] B. Urul, "Gain enhancement of microstrip antenna with a novel DNG material," *Microw. Opt. Technol. Lett.*, vol. 62, no. 4, pp. 1824–1829, Apr. 2020.

[65] H. Suthar, D. Sarkar, K. Saurav, and K. V. Srivastava, "Gain enhancement of microstrip patch antenna using near-zero index metamaterial (NZIM) lens," in *Proc. 21st Nat. Conf. Commun. (NCC)*, Mumbai, India, Feb. 2015, pp. 1–6.

[66] Y. Guo, J. Zhao, and X. Zhao, "A novel high-gain omnidirectional antenna using near-zero-index metamaterials," *Microw. Opt. Technol. Lett.*, vol. 64, no. 7, pp. 1280–1287, Jul. 2022.

[67] M. Moniruzzaman, M. T. Islam, N. Misran, M. Samsuzzaman, T. Alam, and M. E. H. Chowdhury, "Inductively tuned modified split ring resonator based quad band epsilon negative (ENG) with near zero index (NZI) metamaterial for multiband antenna performance enhancement," *Sci. Rep.*, vol. 11, no. 1, p. 11950, Jun. 2021.

[68] A. Bakhtiari, "Investigation of enhanced gain miniaturized patch antenna using near zero index metamaterial structure characteristics," *IETE J. Res.*, vol. 68, no. 2, pp. 1312–1319, Mar. 2022.

[69] J. Lee, H. Kim, and J. Oh, "Large-aperture metamaterial lens antenna for multi-layer MIMO transmission for 6G," *IEEE Access*, vol. 10, pp. 20486–20495, 2022.

[70] R. K. Luneburg, *Mathematical Theory of Optics*. Berkeley, CA, USA: Univ. California Press, 1966.

[71] D. C. Kampouridou, T. D. Karamanos, A. I. Dimitriadis, and N. V. Kantartzis, "Metamaterial-based 3D Luneburg lens antenna design for microwave frequencies," in *Proc. 10th Eur. Conf. Antennas Propag. (EuCAP)*, Davos, Switzerland, Apr. 2016, pp. 1–5.

[72] Z. Yang, L. Guo, C. Yao, Q. Zhang, Z. Xu, M. Guo, and Z. Wang, "Ultrawideband antipodal tapered slot antenna with gradient refractive index metamaterial lens," *IEEE Antennas Wireless Propag. Lett.*, vol. 18, pp. 2741–2745, 2019.
[73] Z. Szabó, G.-H. Park, R. Hedge, and E.-P. Li, "A unique extraction of metamaterial parameters based on Kramers–Kronig relationship," *IEEE Trans. Microw. Theory Techn.*, vol. 58, no. 10, pp. 2646–2653, Oct. 2010.
[74] Q.-W. Lin, Y.-S. To, and H. Wong, "A dual-polarized lens antenna using gradient refractive index (GRIN) metasurface," in *Proc. IEEE Asia–Pacific Microw. Conf. (APMC)*, Hong Kong, Dec. 2020, pp. 1063–1065.
[75] R. Singha and D. Vakula, "Directive beam of the monopole antenna using broadband gradient refractive index metamaterial for ultra-wideband application," *IEEE Access*, vol. 5, pp. 9757–9763, 2017.

MD MIRAZUR RAHMAN received the B.S. degree in electrical, electronic, and communication engineering from the Military Institute of Science and Technology, Bangladesh, in 2007, and the M.S. degree in wireless networks from the Queen Mary University of London, U.K., in 2009. He is currently pursuing the Ph.D. degree in electrical and computer engineering with North Dakota State University, Fargo, ND, USA. Since 2022, he has been a Research Assistant with the RF Connect Laboratory, Department of Electrical and Electronic Engineering, North Dakota State University. His research interests include the development of metamaterial assisted phased array antennas for satellite based the IoT applications, chipless, and chip-based RFID sensors for healthcare and precision agriculture. His awards and honors include the Fellowship from North Dakota Water Resources Research Institute (NDWRRI), and research grant from United States Department of Agriculture (USDA).

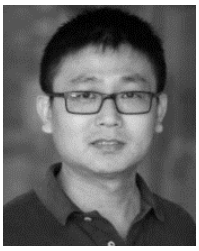

YANG YANG (Senior Member, IEEE) was born in Bayannur, China. He received the Ph.D. degree from Monash University, Melbourne, VIC, Australia, in 2013. He has three years of industry experience with Rain Bird Australia serving as an Asia-Pacific GSP Engineer, from 2012 to 2015. In April 2015, he returned to academia working in the field of microwave and antenna technologies, with the Centre for Collaboration in Electromagnetic and Antenna Engineering, Macquarie University. In April 2016, he was appointed a Research Fellow with the State Key Laboratory of Terahertz and Millimeter Waves, City University of Hong Kong. In December 2016, he joined the University of Technology Sydney, Australia. He is currently a Senior Lecturer and a Team Leader in millimeter-wave integrated circuits and antennas. He has more than 150 international peer-reviewed publications in microwave and millimeter-wave circuits and antennas. He received the Corporate 2014 Global GSP Success Award (one globally). He is a Global Winner of the CST University Publication Award 2018, by CST, Dassault Systems. He is an Associate Editor of IEEE Access, and an Area Editor of *Microwave and Optical Technology Letters*.

SHUVASHIS DEY (Member, IEEE) received the Bachelor of Technology (B.Tech.) degree in electronics and communication engineering from the National Institute of Technology, Durgapur, West Bengal, India, in 2007, the M.Sc. degree in wireless networks (physical pathway) from the Queen Mary University of London, U.K., in 2009, and the Ph.D. degree in electrical and computer systems engineering from Monash University, Australia, in 2018. He is currently an Assistant Professor with the Department of Electrical and Computer Engineering, North Dakota State University. He was a Postdoctoral Research Fellow with the Department of Electrical and Computer Systems Engineering, Monash University, from 2019 to 2021. He was also a Research Affiliate with the Auto-ID Labs, Massachusetts Institute of Technology (MIT), Cambridge, MA, USA, from 2016 to 2020. His research interests include microwave devices and antennas, wearable antennas for healthcare applications, metamaterials and metasurface, and chipless and chip-based UHF RFID tags and sensors. His awards and honors include the Young Scientist's Travel Grant at the IEEE International Symposium on Antennas and Propagation (ISAP), in 2012, the IEEE MTT-S Ph.D. Student Sponsorship Initiative Award, in 2016, and the Best Presentation Award at the International Conference on Sensing Technology (ICST) 2017.